Erythroid overproduction of erythroferrone causes iron overload and developmental abnormalities in mice

Richard Coffey[1], Grace Jung[1], Renata C. Pereira[3], Elizabeta Nemeth[1] and Tomas Ganz[1, 2]

Departments of Medicine[1], Pathology[2] and Pediatrics[3], David Geffen School of Medicine at UCLA

Los Angeles, California 90095, USA

Corresponding Author: Tomas Ganz, PhD, MD

E-mail: tganz@mednet.ucla.edu

Abstract

The hormone erythroferrone (ERFE) is produced by erythroid cells in response to hemorrhage, hypoxia or other erythropoietic stimuli, and suppresses the hepatic production of the iron-regulatory hormone hepcidin, thereby mobilizing iron for erythropoiesis. Suppression of hepcidin by ERFE is thought to be mediated by interference with paracrine BMP signaling that regulates hepcidin transcription in hepatocytes. In anemias with ineffective erythropoiesis, ERFE is pathologically overproduced but its contribution to the clinical manifestations of these anemias is not well understood. We generated three lines of transgenic mice with graded erythroid overexpression of ERFE and showed that they developed dose-dependent iron overload, impaired hepatic BMP signaling and relative hepcidin deficiency. At the highest levels of ERFE overexpression the mice manifested decreased perinatal survival, impaired growth, small hypofunctional kidneys, decreased gonadal fat depots and neurobehavioral abnormalities, all consistent with impaired organ-specific BMP signaling during development. Neutralizing excessive ERFE in congenital anemias with ineffective erythropoiesis may not only prevent iron overload but may have additional benefits for growth and development.

Introduction

Systemic iron homeostasis is tightly regulated by the hepatic hormone hepcidin, which inhibits intestinal iron absorption and the mobilization of stored iron [1]. Erythropoietic activity, dependent on adequate iron supply, strongly influences iron homeostasis. During physiological response to anemia, within hours after erythropoietin (EPO) induction, hepcidin is suppressed [2], increasing iron flows into blood plasma and iron delivery to the marrow to support the enhanced production of erythrocytes. In anemias with ineffective erythropoiesis, in which EPO levels are increased and the erythropoietic compartment is disproportionately expanded, hepcidin is pathologically suppressed [3,4] resulting in excessive iron absorption and eventual iron overload, even in patients who are not receiving blood transfusions. The search for factors that suppress hepcidin in response to increased erythropoiesis[5] led to the discovery of erythroferrone (ERFE), a hormone produced by erythroblasts that acts on the liver to suppress hepcidin expression by hepatocytes [6].

Recent studies provided evidence that ERFE inhibits hepcidin expression by antagonizing select members of the bone morphogenetic protein (BMP) family [7,8]. BMP2/6 signaling in hepatocytes regulates hepcidin transcription in response to plasma iron concentrations and hepatic iron stores, and the pathological loss of BMP signaling causes hepcidin deficiency and systemic iron overload [9,10]. ERFE lowers hepcidin transcription by sequestering the BMP2/6 heterodimer secreted by the sinusoidal endothelial cells [8], but ERFE is also reported to bind other BMPs including BMP2, 4, 5, 6 and 7 [7,11]. Considering the pleiotropic effects of BMP, the endocrine effects of pathologically-increased ERFE need not be limited only to altered hepcidin regulation in the liver.

Although substantial evidence supports the role of ERFE as a stress hormone that acutely suppresses hepatic hepcidin synthesis in response to erythropoietic stimuli, much less is known about the chronic effects of ERFE *in vivo*. The effect of chronically elevated ERFE levels have been analyzed in the context of erythropoietic disorders such as β-thalassemia [12]. However, while patients with β-thalassemia commonly suffer from problems that could be linked to disruptions in BMP signaling, including iron overload [13], renal impairment [14], and skeletal problems such as impaired growth [15] or bone mineralization [16], it is unclear to which extent the observed pathologies are attributable to elevated ERFE as opposed to other factors such as tissue and organ hypoxia, the effects of hemolytic products or the toxicity of treatment. Animal models of increased ERFE production depend on the stimuli of anemia [17,18] or EPO administration [19] but serum ERFE levels in these models are orders of magnitude lower than in human patients with β-thalassemia [12]. Additionally, high EPO levels exert multiple systemic effects [20] beyond increasing *Erfe* expression and these complicate direct attribution of observed phenotypes to the action of ERFE alone .

The aim of the current study was to determine the effect of chronically elevated *Erfe* expression on systemic iron homeostasis and BMP signaling, independently of the effects of chronic anemia or EPO treatment and at a range of circulating ERFE levels similar to those present in humans with β-thalassemia and other anemias with ineffective erythropoiesis. To this end we generated multiple lines of novel transgenic mice overexpressing graded levels of erythroferrone in erythroid cells. We find that chronically elevated *Erfe* expression results in dose-dependent hepcidin suppression, dysregulation of iron homeostasis and tissue iron accumulation. Additionally, at high levels, chronic *Erfe* overexpression affects multiple organ systems influencing pup survival, kidney function, and behavior.

Materials and Methods

Transgenic mice

A DNA construct previously shown to target gene overexpression to erythroid cells was generously contributed by Dr. Kenneth R. Peterson [21] and adapted to express N-FLAG-*mErfe* **(Figure 1A).** Transgenic founder animals were generated at Cyagen labs by pronuclear injection of fertilized C57BL/6N zygotes. One transgenic founder generated by this method gave rise to the high-expressing “H” line and the moderately expressing “M” line, and the second transgenic founder gave rise to the low-expressing “L” line. Individual transgenic lines were established and experimental mice generated by breeding heterozygous transgenic mice with C57BL/6J mice to yield transgenic mice and WT littermate controls. Each mouse was genotyped to ensure stability of transgene copy number.

Animal Husbandry

Animals were fed a natural ingredient diet (Labdiet 5053) containing ~220 ppm iron and housed in a specific-pathogen-free barrier facility. Animal body weights were recorded weekly beginning at 3 weeks and until euthanasia, either at 6 or 16 weeks of age. Experimental animals were euthanized by isoflurane inhalation. All experiments involving mice were conducted with the approval of the University of California, Los Angeles Animal Research Committee.

Genomic characterization

Genomic DNA was prepared from the livers of the H-line transgenic founder, H-line F1 progeny, M-line founder, and one M-line F1 progeny using Qiagen Gentra Purgene kit per manufacturer's instructions. Genomic sequencing on paired-end libraries was performed at UCLA Technology Center for Genomics & Bioinformatics using an Illumina Novaseq S4 DNA sequencer. The reads were aligned to the reference genomic sequence Mus musculus strain C57BL/6J chromosome 4, GRCm38.p6 C57BL/6J and to the transgene sequence, and overlap sequences between adjacent transgene copies and between transgene and chromosomal sequence identified and used to ascertain the chromosomal insertion site, and transgene copy number.

Measurement of iron-related and hematological parameters

Serum iron and liver non-heme iron were measured by using a colorimetric assay according to the manufacturer's protocol (Sekisui Diagnostics). Prior to sampling, livers were homogenized to reduce variation resulting from regional differences in hepatic iron deposition. Hemoglobin levels, red-blood-cell counts, and hematocrit % were determined by using a HemaVet blood analyzed (Drew Scientific).

Quantification of serum and urinary proteins and metabolites

Serum ERFE concentrations were determined as previously described [18] with the substitution of DELFIA europium-conjugated streptavidin for horseradish peroxidase conjugated streptavidin. Fluorescence was measured by CLARIOstar plate reader. Serum hepcidin concentrations were determined by ELISA as detailed previously [6]. Serum urea nitrogen concentrations were measured by using the QuantiChrom Urea Assay Kit (BioAssay Systems), urinary albumin using the Mouse Albumin ELISA Kit (Abcam, ab108792) and urinary creatinine using the Creatinine (urinary) Colorimetric Assay Kit (Cayman Chemical), all in accordance with the manufacturers' protocols.

RNA isolation and measurement of gene expression

Total RNA isolation was performed by using TRIzol (ThermoFisher Scientfic). cDNA was synthesized using the iScript cDNA Sythesis Kit (Bio-Rad) following the manufacturer's protocol. Relative mRNA expression for genes of interest were determined by quantitative RT-PCR using SsoAdvanced Universal SYBR Green Supermix (Bio-Rad) and measured on a CFX-96 RT-PCR Detection System (Bio-Rad). Primer sequences used in this study are listed in Supplemental Table 1.

Behavioral testing

All behavioral testing was performed at the UCLA behavioral testing core facility by personnel blinded to the mouse genotype. Mice were transferred to the testing facility and allowed 1 week to acclimate prior to testing between 11 and 13 weeks of age. Open-field testing was performed for a duration of 30 minutes in an empty and dimly lit, light intensity less than 20 lux, square area measuring 30 cm per side. Mouse movement was recorded automatically and analyzed by using ANY-maze software (Stoelting). Righting reflex of experimental animals was assessed by flipping animals held by the tail, so that the animal passed through an inverted position, to an approximate height of 25 cm. Landing position of the mouse was recorded and a score of 0, 1, or 2 given to mice that landed on their feet (0), side (1), or back (2), respectively. Righting reflex testing was performed three times per mouse and the highest value recorded. Negative geotaxis testing was assessed by placing mice facing downwards on a declined surface. Mouse movement was recorded for a duration of 30 s and a score of 0, 1, 2, or 3 was given to mice that turned to face upslope and climbed (0), turned without climbing (1), moved without turning (2), or did not move (3). Reaction to auditory stimulation was measured by the degree of visible

response to a 20 KHz sound with a volume of 90 dB at mouse location. A score of 0, 1, 2, or 3 was given to mice that did not respond (0), exhibited a pinna reflex (1), jumped < 1 cm (2), or jumped > 1 cm (3). Wire maneuvering capacity was assessed by the ability of mice to hang onto a wire and navigate to an attachment post when allowed to initially establish a foreleg grip. A score of 0, 1, 2, 3, or 4 was assigned to mice that demonstrated active hindleg grip (0), impaired hindleg grip (1), inability to grip with hindlegs (2), inability to lift legs followed by falling (3), or immediately falling (4).

Bone histomorphometry analysis

Mouse femurs were dehydrated and fixed in 70% ethanol prior to embedding in methyl methacrylate. Sections cut longitudinally at a thickness of 5 µm were stained with toluidine blue (pH 6.4) and used for static bone parameter analysis on a total of 20 fields per sample by using a OsteoMeasure morphometry system (Osteometics, Atlanta) at a distance of 200 µm from the growth plate. Results for individual parameters are listed using accepted units and terminology recommended by the Histomorphometry Nomenclature Committee of the American Society for Bone and Mineral Research [22].

Statistical analysis

Statistical analysis was performed by using the statistical package included in Prism version 8 (GraphPad). $P<0.05$ was considered statistically significant. For each individual transgenic mouse line and its WT littermates, means of experimental groups, defined by genotype and sex, were compared with others by using either student's *t*-test, Welch's ANOVA, or Two-way ANOVA where indicated. In the event of significant differences between group means after one-way ANOVA analysis, individual group means were compared by using an unpaired-*t*-test with Welch's correction. Significant interaction between variables during two-way ANOVA testing was followed by Šidak's multiple comparisons test to determine significant differences between WT and transgenic mice within each sex. Analysis of observed vs expected ratios when analyzing transgene inheritance was performed by using binomial testing and an expected transgene incidence of 50%. Fisher's exact test was used to analyze differences in phenotypic incidence between groups. In behavioral analysis, to identify outliers in a group of mice, ROUT analysis (Prism version 8, GraphPad) was performed with a false discovery rate set at 0.1%.

Results

Generation of Erfe-overexpressing mice

We generated mice that selectively overexpress *Erfe* in erythroid cells by pronuclear injection with a transgene construct that placed *Erfe* expression under the control of an erythroid-specific promoter-enhancer **(Figure 1A)**. The three lines of transgenic mice differed in the degree of *Erfe* overexpression and were designated as high (line-H), medium (line-M), and low (line-L) *Erfe*-overexpressing mice, but all had elevated bone marrow *Erfe* expression relative to wild-type (WT) littermates **(Figure 1B)**. Lines H and M had been derived from the highest-expressing founder. Genomic sequencing identified the haploid transgene insertion site on Chr. 4, from 11985998 to 12010497, overlapping into gene 1700123M08Rik noncoding RNA of unknown function. The H and M lines differed by transgene copy number (3 vs 1), resulting from a rare spontaneous deletion of 2 tandem copies of the transgene. Line-L was derived from another founder and was not further genomically characterized. Transgene expression was similar at 6- and 16-week time points **(Figure 1B, C)**.

Serum ERFE levels in line-L transgenic mice were near the threshold of detection by ELISA, below levels previously measured in WT mice after EPO injection or in $Hbb^{Th3/+}$ thalassemic mice [18]. Compared with line-L, serum ERFE levels were ~20x higher in line-M and ~200x in line-H transgenic mice **(Figure 1D).** Interestingly, moderate differences in mRNA bone marrow *Erfe* expression led to much larger differences in circulating ERFE levels between transgenic lines **(Figure 1E)**.

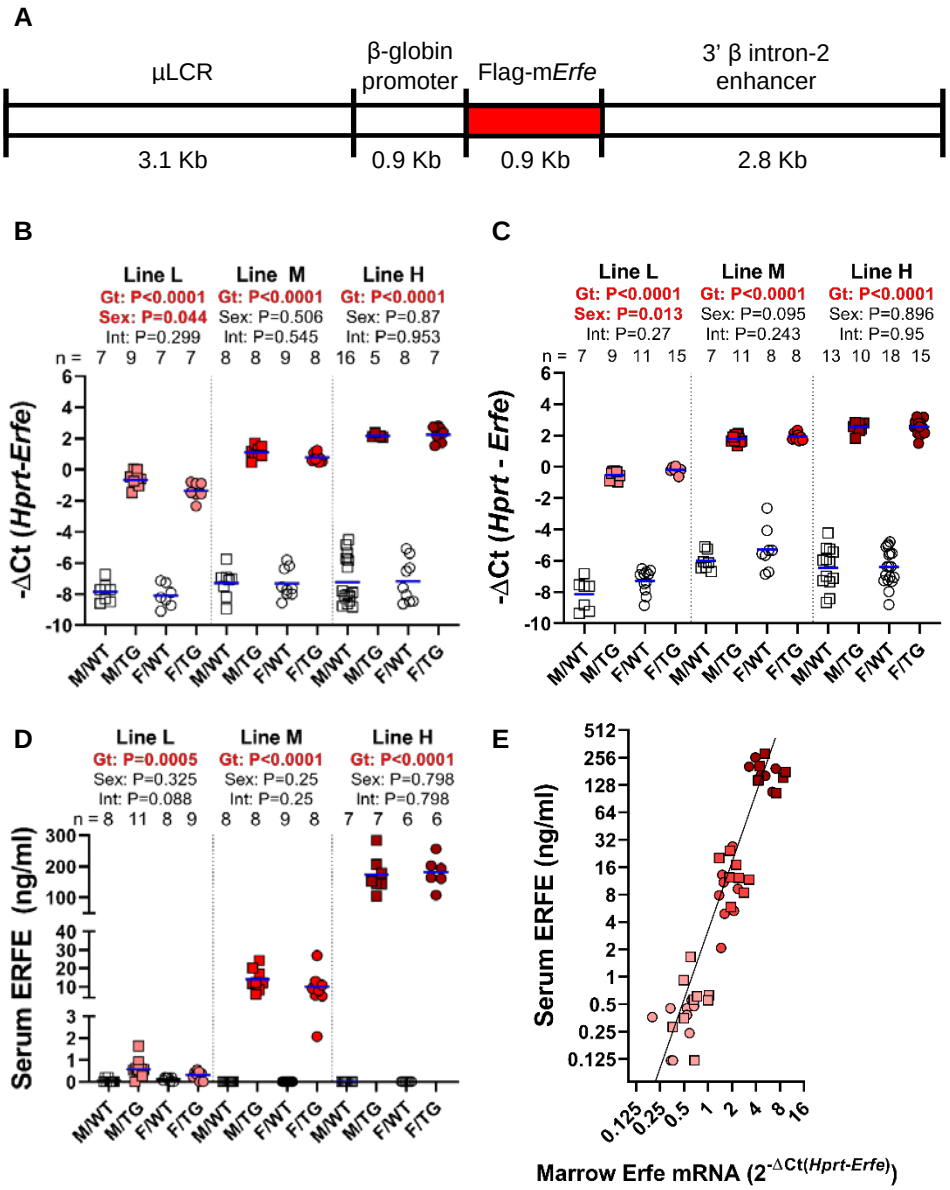

Figure 1. Generation of Hbb-*Erfe* mice and analysis of *Erfe* overexpression. A) Structure of the transgene construct. Bone marrow *Erfe* mRNA in **B**) 6 week-old and **C**) 16-week old mice. **D)** Serum ERFE levels of 6-week-old mice, **E**) Relationship between serum ERFE protein levels and marrow *Erfe* mRNA, regression line $Y=3.19^* X^{2.5}$ (r^2 =0.51). In all panels, male (M, square) and female (F, round); mean of each group is shown by blue line, TG = *Erfe*-overexpressing mice (line-L pink, line-M red, and line-H dark red symbols) and WT = WT littermate controls (white symbols). Within each individual transgenic line, groups were compared by two-way ANOVA to determine significant effects (P<0.05, bold red) of genotype and sex on data variation and to identify interactions between these variables. Cohort numbers for mRNA and serum analysis are shown.

Erfe overexpression causes iron overload and elevated hemoglobin levels

Erfe overexpression dose-dependently increased liver non-heme iron levels. At 6 weeks of age, transgenic mice from lines L, M and H respectively loaded ~2, ~3.6 and ~4.2 times more liver non-heme iron than their WT littermates **(Figure 2A)**. The effect of elevated *Erfe* expression on liver iron accumulation persisted in 16-week-old transgenic mice **(Figure 2B)**. Females had higher liver iron levels than males, consistent with the previously described sex differences in iron loading of the C57BL/6 strain [23]. Serum iron was also elevated in both male and female transgenic mice from line-M and H, but not line-L, at 6 weeks of age **(Figure 2C),** and elevated in transgenic mice aged 16 weeks in all lines relative to WT littermates **(Figure 2D)**.

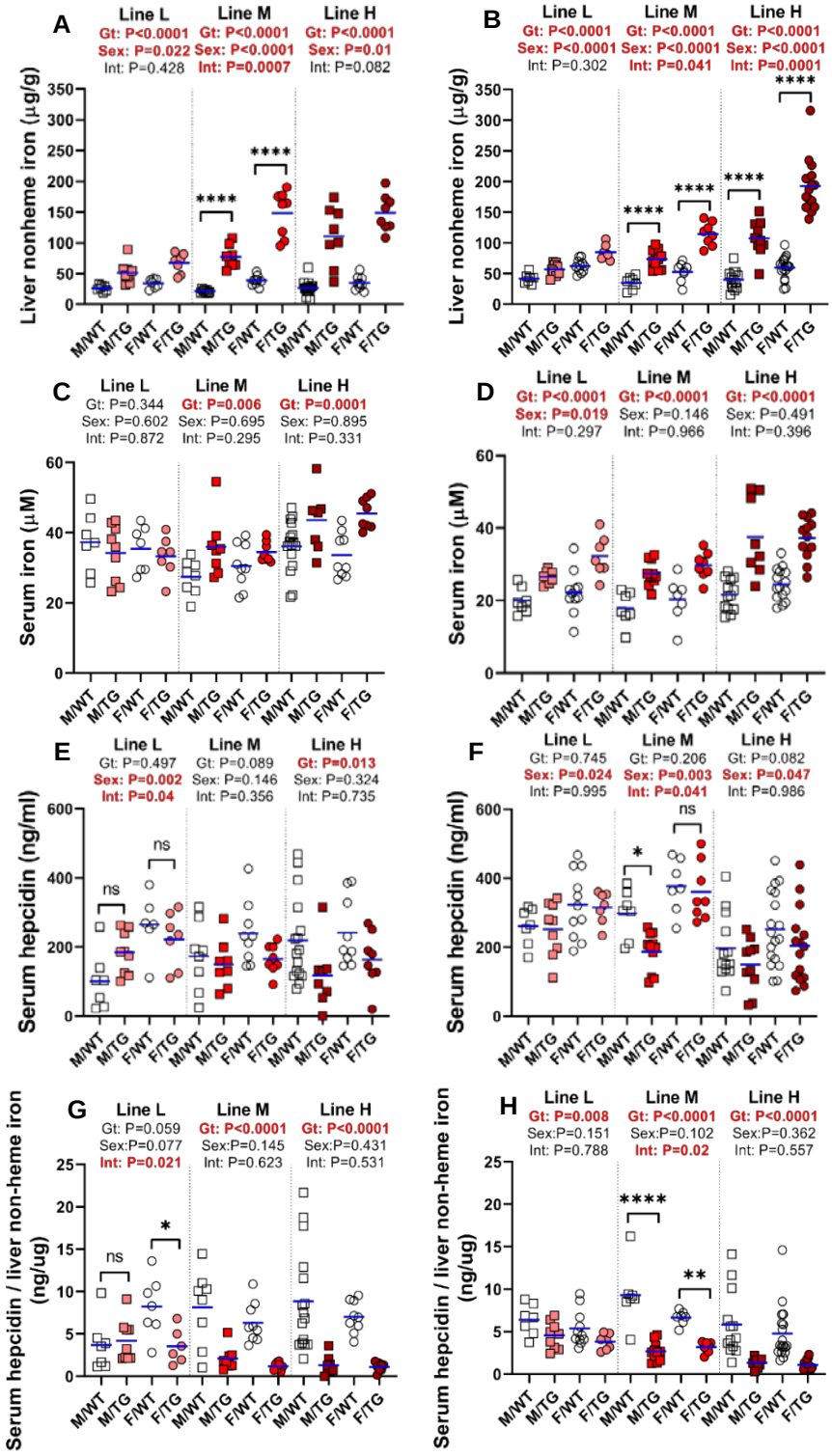

Figure 2. *Erfe* overexpression causes dose-dependent iron accumulation and inadequate hepcidin expression. Liver non-heme iron (**A, B**), serum iron (**C, D**), serum hepcidin (**E, F**), and serum hepcidin relative to liver iron (**G**, **H**) levels at 6 (**A, C, E, G**) and 16 (**B, D, F, H**) weeks of age in male (M) and female (F) *Erfe*-overexpressing (TG) mice and WT (WT) littermate controls from line-L (white/pink), line-M (white/red), and line-H (white/dark red); mean of each group is shown in blue. For each mouse line, groups were compared by two-way ANOVA to determine effects of genotype and sex on data variation (significant differences denoted in bold red) and to identify interactions between these variables. In the event of significant interaction between genotype and sex, individual groups were compared by Šidak's multiple comparisons test (ns=P≥0.05, *=P<0.05, **=P<0.01, ***=P<0.001, ****=P<0.0001).

Serum hepcidin concentrations in *Erfe*-transgenic mice would be expected to be determined by the balance between the suppressive effect of ERFE on hepcidin synthesis and the stimulatory effect of increased hepatic

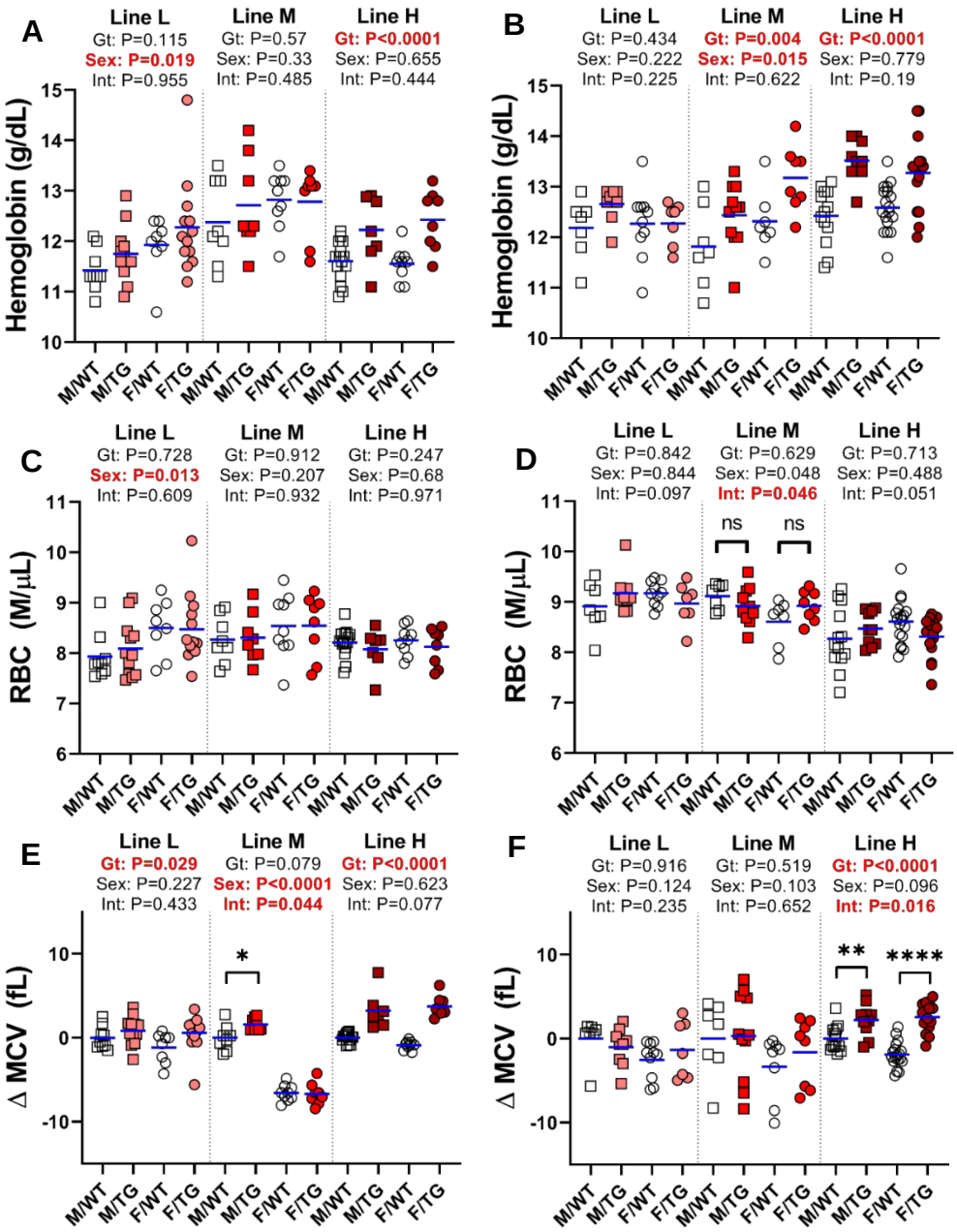

Figure 3: ERFE enhances erythropoiesis in a dose-dependent manner. Hemoglobin levels (**A**, **B**), red blood cell (RBC) counts (**C, D**), and differences in MCV relative to male WT (WT) littermates (**E**, **F)** at 6 (**A, C, E**) and 16 (**B, D, F**) weeks of age in male (M) and female (F) *Erfe*-overexpressing (TG) mice and WT littermate controls from line-L (white/pink), line-M (white/red), and line-H (white/dark red); mean of each group is shown in blue. Groups within each individual line were compared by two-way ANOVA to determine significant effects of genotype and sex on data variation and to identify interactions between these variables (P<0.05 denoted in bold red). In the event of significant interaction between genotype and sex, individual groups were compared by Šidak's multiple comparisons test (NS=P≥0.05, *=P<0.05, **=P<0.01, ***=P<0.001, ****=P<0.0001).

and plasma iron concentrations [24,25]. In line-L transgenic mice at 6 or 16 weeks of age, serum hepcidin concentrations were similar to those of WT mice **(Figure 2E, F)**, consistent with these transgenic mice reaching iron balance by 6 weeks. In line M, the mean serum hepcidin concentrations were lower in transgenic than WT mice but this reached statistical significance only in males at 16 weeks. In line-H, hepcidin was significantly suppressed in both sexes at 6 weeks. Importantly, the ratio of serum hepcidin concentrations to liver non-heme iron content was lower in transgenic than WT mice, indicating inappropriately low hepcidin production relative to the severity of iron loading, with the exception of line-L males at 6 weeks **(Figure 2G, H)**.

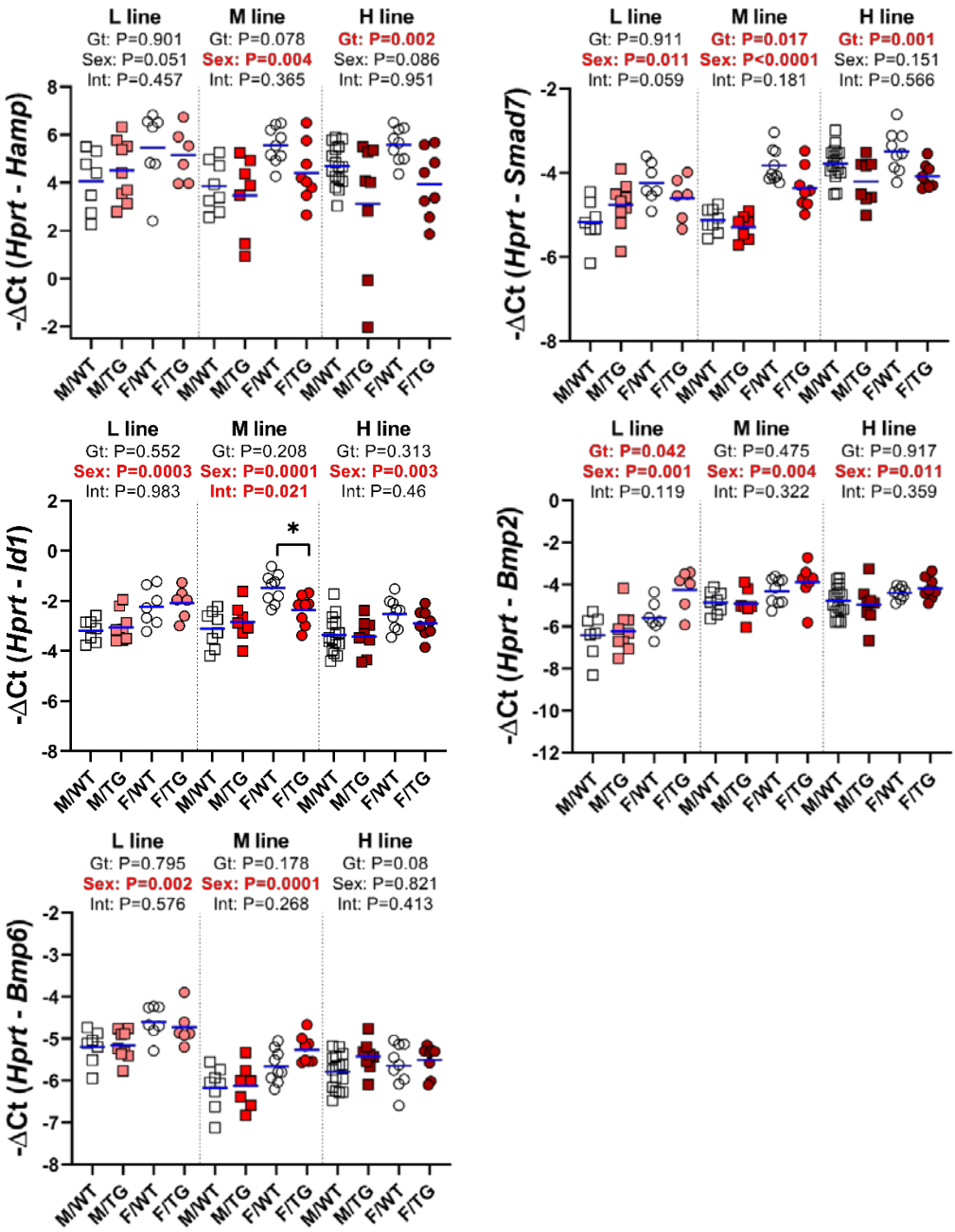

Figure 4. Effect of *Erfe* overexpression on liver BMP signaling. Relative mRNA expression of **A)** *Hamp*, **B)** *Smad7*, **C)** *Id1*, **D)** *Bmp2* and **E)** *Bmp6* in the liver at 6 weeks of age in male (M) and female (F) *Erfe*-overexpressing (TG) mice and WT (WT) littermate controls from line-L (white/pink), line-M (white/red), and line-H (white/dark red); mean of each group is shown in blue. Groups within each individual line were compared by two-way ANOVA to determine significant effects of genotype and sex on data variation and to identify interactions between these variables (P<0.05 denoted in bold red). In the event of significant interaction between genotype and sex, individual groups were compared by Šidak's multiple comparisons test (NS=P≥0.05, *=P<0.05, **=P<0.01, ***=P<0.001, ****=P<0.0001).

At both 6 and 16 weeks of age, transgenic mice from line-H had elevated hemoglobin levels **(Figure 3A, B)** but not RBC counts **(Figure 3C, D),** and their erythrocytes were larger **(Figure 3E, F).** We did not detect consistent differences in hematological parameters between transgenic and WT mice in the M or L line.

Tissue-selective effect of Erfe overexpression on BMP signaling

The high concentration of erythroid *Erfe*-overexpressing cells in the bone marrow raised the possibility that ERFE may locally suppress BMP signaling[7,11] in that organ. However, we found no suppressive effect of ERFE on the

expression of the BMP target genes *Smad7* or *Id1* at 6 weeks of age **(Figure S1A-B),** and *Bmp2* or *Bmp6* expression in the bone marrow was also not affected **(Figure S1C-D).**

In the liver, we detected a suppressive effect of higher ERFE concentrations on the hepatic expression *Hamp* and *Smad7* but not *Id1* **(Figure 4A-C)**. There was no effect of *Erfe* overexpression on the hepatic mRNA levels of *Bmp2* and *Bmp6* **(Figure 4D-E)**.

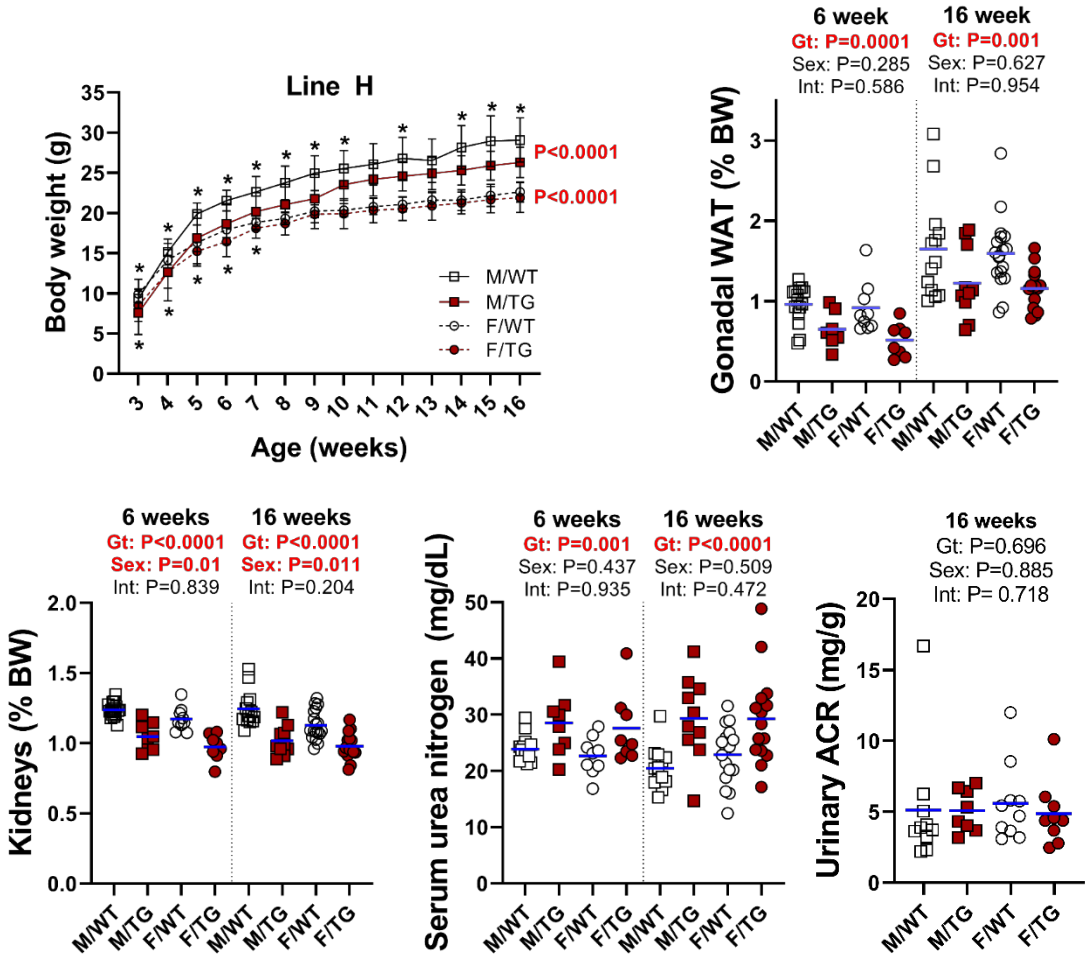

Figure 5. High *Erfe* expression causes reduced body and kidney mass in line-H mice. A) Growth curves from ages 3 to 16 weeks of age. Statistical significance of the effect of genotype on data variation between body weights of sex-matched wild type (WT) and transgenic (TG) mice determined by 2-way ANOVA are displayed to the right of their respective curves. Statistically significant differences (P<0.05) between sex-matched WT and TG body weights at individual time points, determined by Student's *t*-test, are indicated by asterisks (*) above or below curves for males and females, respectively. **B)** Decreased mass of gonadal white adipose tissue (WAT) pads and **C**) kidneys from line-H mice as a percentage of total body weight at 6 and 16 weeks of age. **D**) Serum blood urea nitrogen (BUN) in line-H mice at 6 and 16 weeks of age and **E**) urinary albumin-creatinine ratio (ACR) in line-H mice at 16 weeks of age. Groups at each age were compared by two-way ANOVA to determine significant effects of genotype and sex on data variation and to identify interactions between these variables (P<0.05 denoted in bold red). In the event of significant interaction between genotype and sex, individual groups were compared by Šidak's multiple comparisons test (NS=P≥0.05, *=P<0.05, **=P<0.01, ***=P<0.001, ****=P<0.0001).

Erfe overexpression affects growth and organ size

We next surveyed for potential effects of ERFE on morphogenesis and homeostasis in other tissues. Male transgenic mice from line-H had consistently reduced body weights, compared with WT littermates, between the ages of 3 and 16 weeks **(Figure 5A).** Female transgenic mice from Line-H also weighed less than WT but the difference resolved with age. Transgenic mice from line-M were also lighter than their WT littermates, again with larger differences in males than females **(Figure S2A)**. Transgenic mice from line-L, of either sex, weighed the

same as their WT littermates **(Figure S3A)**. Analysis of selected tissues and organs revealed smaller gonadal fat pads and kidneys, even after adjusting for reduced total body weight, in line-H transgenic mice at 6 and 16 weeks of age **(Figure 5B, C).** Smaller kidney size in line-H transgenic mice was associated with reduced kidney function as indicated by elevated serum urea nitrogen levels at 6 and 16 weeks of age **(Figure 5D)**. However, kidney morphology did not appear altered as a result of *Erfe* overexpression in this line and we detected no increase in proteinuria in line-H compared with WT littermates **(Figure 5E)**.

In line-M no differences in individual tissue weights were detected with the exception of lower relative kidney size in line-M transgenic mice compared with WT littermates that was statistically significant in females at 16 weeks of age **(Figure S2B-I)**. No effect of *Erfe* overexpression on tissue or organ weights was detected in line-L mice **(Figure S3B-E)**. Among other tissues analyzed from line-H mice **(Figure S4)**, brain weights from transgenic mice comprised a greater relative proportion of total body weight compared with those of WT littermates **(Figure S4A)**. However, this difference was primarily attributable to the lower body weights of transgenic mice rather than an absolute difference in brain weights. *Erfe* overexpression resulted in significantly reduced inguinal white adipose tissue in 6-week-old, line-H transgenic mice **(Figure S4B)** and increased spleen weights **(Figure S4E)**, relative to total body weights, but these differences were not observed at 16 weeks of age.

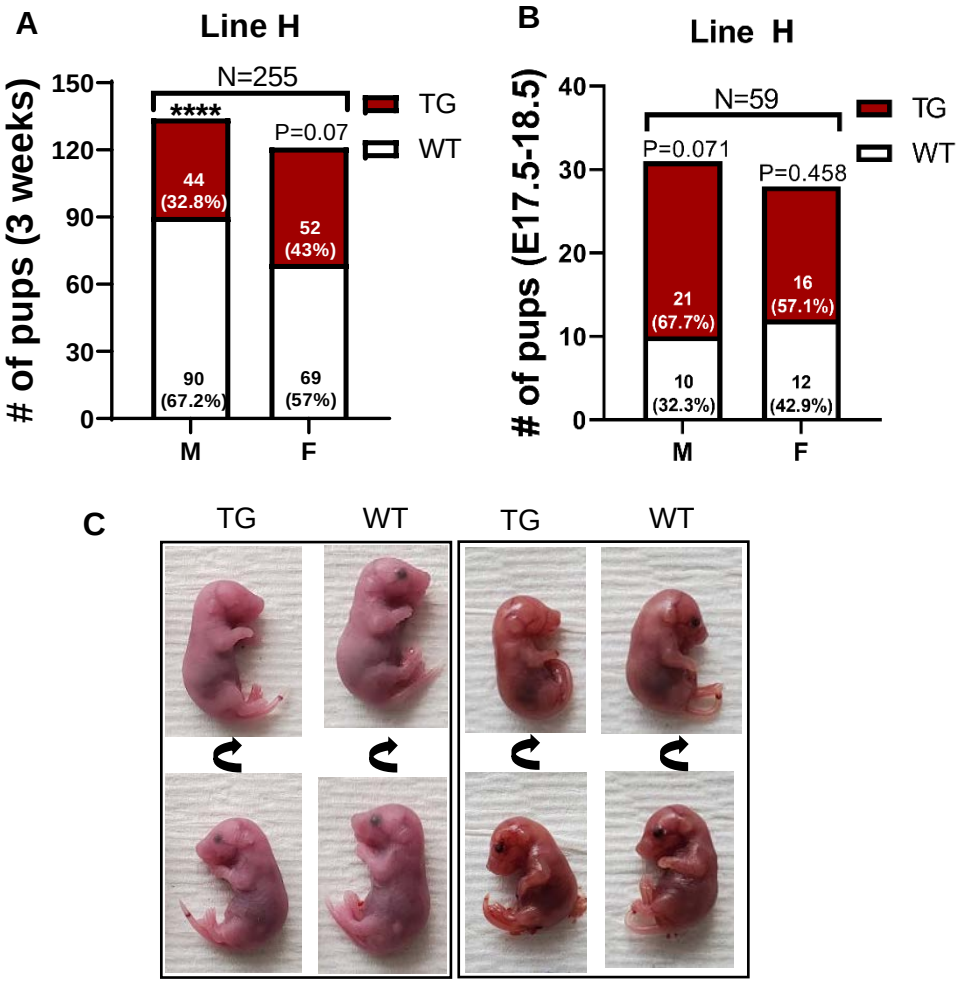

Figure 6. Impaired postnatal survival and unilateral anophthalmia in line-H transgenic mice. Number and within-sex percentage of WT (WT) and transgenic (TG) mice, grouped by sex, from line-H breeding surviving at **A)** 3 weeks of age or **B**) in utero at embryonic day 17.5-18.5. Statistically significant differences from expected proportions were assessed by binomial testing. **C**) Examples of unilateral anophthalmia in line-H TG mice. Top and bottom panels show the same pup rotated to demonstrate, in TG mice, normal (bottom) or impaired (top) eye development compared with WT littermates.

To analyze the effect of erythroid overexpression of *Erfe* on steady-state bone homeostasis (known to be regulated by BMP signaling[26-28]), we performed bone histomorphometry in female line-H mice at 6 weeks of age. We detected no significant differences in any measured parameters of bone development, mineralization, or cell populations **(Table S2)**. Although *Erfe*-overexpressing mice tended to have increased osteoid thickness relative to WT littermates this difference was not statistically significant.

Erfe overexpression impairs pup survival and causes developmental and behavioral abnormalities

The proportion of transgenic mice from line-H surviving to weaning was unexpectedly lower than their WT littermates and was independent of dam genotype. Males were more severely affected with only 32.8% of surviving pups being transgenic ($p<0.0001$), whereas among females 43% of surviving pups were transgenic ($p=0.07$) **(Figure 6A)**. To determine if this divergence from expected mendelian inheritance was attributable to loss of pups during embryonic development, we analyzed genotypes from line-H pups between embryonic day 17.5 and 18.5. The proportion of transgenic to WT embryos did not significantly differ from the expected ratio of 50%, and there was even a nonsignificant trend towards a greater than expected proportion of male embryos being transgenic (**Figure 6B)**. Thus, decreased survival at weaning in the H-line is a result of higher postnatal mortality and not embryonic lethality.

No divergence from expected transgene inheritance ratios was observed in litters from either line-L or line-M breeding (**Figure S5).** Line-H transgenic mice also occasionally presented with permanent eyelid closure of a single eye, occurring in approximately 5% of transgenic mice from this line. Unilateral anophthalmia was seen in developing embryos between days E17.5 and 18.5 in approximately 5% of transgenic mice but not in WT littermates **(Figure 6C)**. Eye abnormalities were not observed in transgenic mice from either line-M or line-L.

Transgenic mice from line-H displayed compulsive circling behavior detectable as early as 3 weeks of age and persistent with aging **(Supplemental video file).** Circling had incomplete penetrance, affecting 38% of line-H transgenic mice with similar incidence in males and females, but was not observed in WT littermates **(Figure 7A)**. Compulsive circling was not observed in transgenic mice from either line-M or L.

We performed a battery of behavioral tests in line-H mice between 11 and 13 weeks of age. During a 30 minute open field test, using automated measurement of mouse movement, mice previously identified as displaying the circling phenotype manifested a greatly increased number of rotations while the remaining transgenic mice exhibited a similar number of rotations as their WT littermates **(Figure 7B)**. Data from male and female mice were combined as analysis by two-way ANOVA indicated no effect of sex on parameters measured during open field testing **(Figure S6)**. By ROUT outlier analysis **(Figure 7B)**, transgenic mice were considered high-circling if they performed more than 150 rotations during open field testing, ~1.5x the highest number of rotations observed in WT mice. Individual high-circling transgenic mice displayed a clear preference for a single direction of rotation **(Figure 7C)**, but as a group had no overall preference for either the clockwise or counter-clockwise direction **(Figure S6A)**. The direction of rotation in individual mice was random in low-circling transgenic mice **(Figure 7C)**. During the open field test high-circling transgenic mice were more active and traveled a greater distance compared with low-circling transgenic mice and WT littermates **(Figure 7D)**. A significant difference in activity between WT and low-circling transgenic mice was also detected, attributable to several low-circling transgenic mice that exhibited a greater amount of rotations during testing than any recorded in WT mice but failed to reach the predetermined threshold to be included in the high-circling group.

To determine if the observed circling phenotype was associated with alterations in vestibular-motor function, we tested the righting reflex and the negative geotaxis response. Line-H mice manifested righting-reflex impairment and a trend towards an impaired negative geotaxis response compared with WT littermates **(Figure S6C, D)**. Compared with WT littermates a significantly higher percentage of line-H transgenic mice displayed impairment in either righting or negative geotaxis **(Figure 7E)**, suggesting that high *Erfe* overexpression is associated with altered vestibular-motor function. *Erfe*-overexpressing and WT mice were equally responsive to auditory stimulation and demonstrated similar physical capacity during a wire maneuver test.

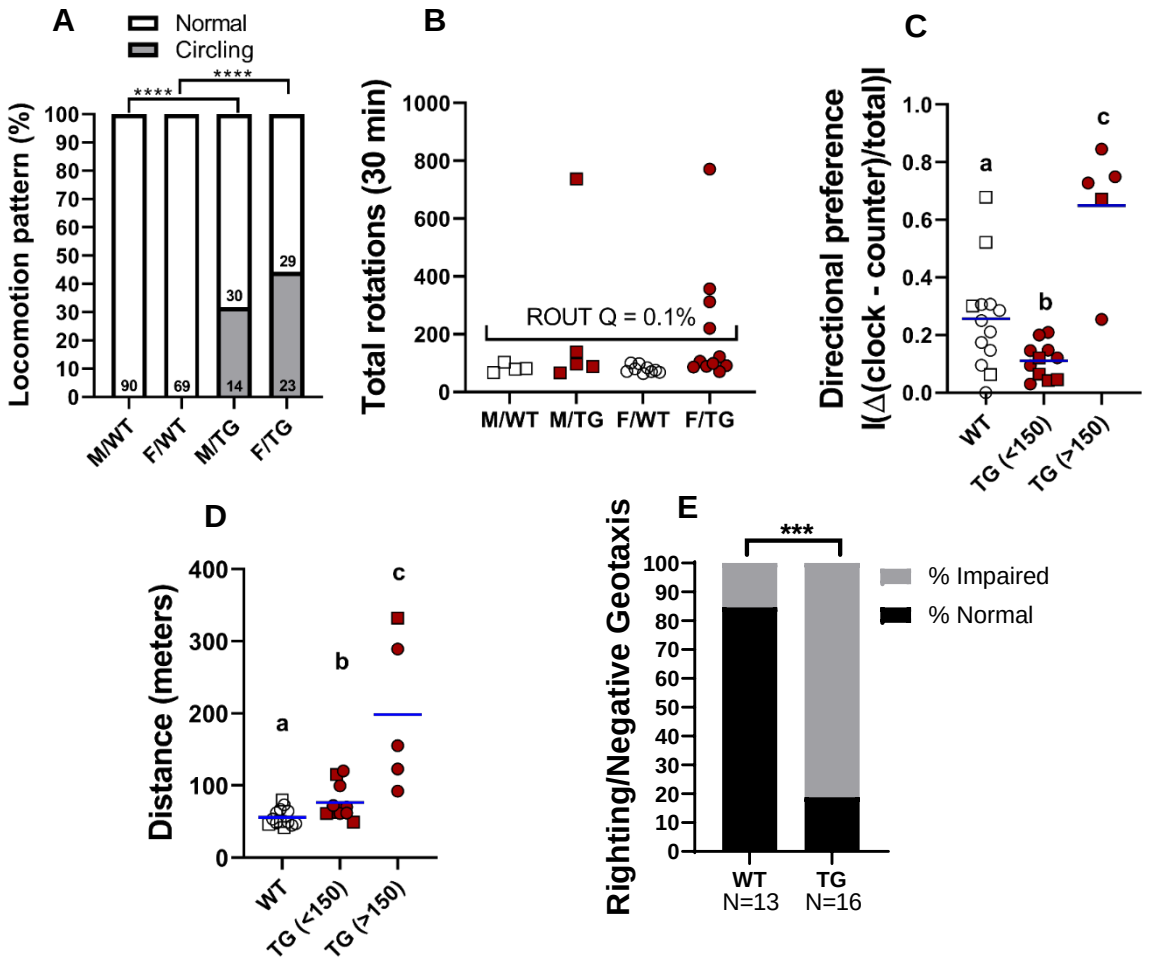

Figure 7. Repetitive circling behavior and impaired motor/vestibular function in line-H transgenic mice. A) Incidence of overt circling behavior in line-H mice. Numerical values on bars indicate animal number per pattern of movement. Statistically significant differences in locomotion pattern between groups of the same sex were determined by Fisher's exact test (****=P<0.0001). **B**) Total rotations completed by mice during open-field testing. Groups were pooled and analyzed for outliers by ROUT test at false discovery rate Q=0.1%. P<0.05 by Fisher exact test for proportion of outliers in TG vs WT mice. **C**) Absolute values of rotation-direction preference and **D)** total distance traveled by line-H mice during open-field testing. Groups of WT mice, TG mice with fewer than 150 rotations during testing (TG (<150)), and TG mice with greater than 150 rotations during testing (TG (>150)) were compared by one-way ANOVA and groups not sharing a common letter superscript are significantly different (P<0.05). **E**) Incidence of impaired outcomes during righting reflex or negative geotaxis testing in line-H mice. A mouse was designated as "impaired" if its combined score from the righting reflex and negative geotaxis testing was >0. Mice categorized as normal had a combined score of 0 on these tests. Statistical significance of the difference in incidence of impairment between groups was determined by Fisher's exact test (***P<0.001).

Discussion

We present evidence that constant, high-level *Erfe* expression by erythroid cells is sufficient to attenuate hepcidin responsiveness to iron loading and to cause systemic iron overload, manifested by increased plasma iron concentrations and hepatic tissue iron stores. Serum ERFE levels in the 3 lines of transgenic mice ranged from ~0.5 ng/ml, similar to levels we measured contemporaneously in $Hbb^{th3/+}$ mice, to ~200 ng/ml, on par with the highest levels reported in humans with β-thalassemia [12]. The large changes in ERFE protein concentrations that result from much smaller changes in *Erfe* mRNA expression suggests decreasing clearance of plasma ERFE at high concentrations. Comparing liver iron content between the 3 transgenic lines indicates that the effect of erythron-derived ERFE on iron loading is dose-dependent but nonlinear.

Liver hepcidin expression is feedback-regulated by liver iron content and serum iron concentrations [11,24]. Any suppression of hepcidin by ERFE will cause increased duodenal iron absorption and hepatic iron accumulation, in turn raising hepcidin concentrations and inhibiting iron absorption, eventually reaching hepcidin concentrations that maintain iron balance. Iron loading in *Erfe*-overexpressing mice changed little between 6 and 16 weeks of age in this study, indicating that by the age of 6 weeks iron balance was reached, a time course similar to that seen in $Hbb^{th3/+}$ mice[29]. The delay in establishment of the iron/hepcidin balance in line-H transgenic mice indicates that higher circulating levels of ERFE require greater accumulation of iron to stimulate hepcidin expression sufficiently to overcome the effects of ERFE. In all transgenic lines, hepcidin levels were inadequate when considered in the context of serum and hepatic iron concentrations.

Line-H *Erfe*-overexpressing mice had elevated blood hemoglobin concentrations at 6 and 16 weeks but not increased erythrocyte numbers, indicative of higher erythrocyte hemoglobin content when compared with WT littermates. Line-M mice also had increased hemoglobin concentrations at 16 weeks but not at 6 weeks when rapid growth stresses the iron supply. These effects are consistent with ERFE-dose-dependent hepcidin suppression and consequently enhanced iron availability, as erythropoiesis in mice and humans is modestly enhanced by hepcidin suppression and increased iron availability [30,31]. Paradoxically, in the mouse model of β-thalassemia hepcidin suppression and increased iron supply worsen ineffective erythropoiesis and anemia, as shown by improved hemoglobin concentrations after interventions that increase hepcidin [32,33]. A recent report of the detrimental effects of a genetic *Erfe* variant that increased ERFE production in congenital dyserythropoietic anemia type II supports the possibility that chronically elevated ERFE production and the resulting excess of iron may also worsen anemia in human disorders of ineffective erythropoiesis [34].

We examined our model for evidence that the effects of ERFE were mediated by suppression of BMP signaling. Although specifics of the interaction between ERFE and individual BMPs may vary by species [35], ERFE is reported to interact with BMP2, 4, 5, 6, 7, and a heterodimer of BMP2/6 [7,8,11]. We assessed the expression of the BMP-responsive genes *Id1* [36] and *Smad7* [37] in the liver, a peripheral tissue responsive to ERFE, as well as the bone marrow, a population of cells that could be subject to the autocrine or paracrine effects of erythroid-derived ERFE. In the liver we identified a suppressive effect of moderate or high *Erfe* overexpression on *Smad7*, but not *Id1* expression. We did not detect a decrease in the expression of *Id1* or *Smad7* in the bone marrow of *Erfe*-overexpressing mice compared with WT littermates. This lack of effect is unlikely to be attributable to a compensating increase in BMP expression by cells in the marrow as expression of *Bmp2* and *Bmp6* did not show a dose-dependent trend towards increased expression across lines of *Erfe*-overexpressing mice. Differential sensitivity of tissues to the effects of ERFE suggests that the mechanism of ERFE action may depend on differences in local BMP signaling mechanisms.

While the abnormalities in transgenic mice with low to moderate circulating levels of ERFE were almost entirely limited to iron homeostasis, line-H transgenic mice displayed increased postnatal mortality, reduced body weight and gonadal adipose tissue weight, reduced kidney size and function, occasional unilateral anophthalmia, and compulsive circling behavior. We considered the possibility that the multiple abnormalities in line-H were caused by disruption of a critical gene at the site of transgene insertion. However, we found no evidence for this possibility by genomic sequencing. Line-H is derived from the same founder as line-M and shares the same insertion site on Chr. 4 overlapping a gene for a noncoding RNA of unknown function, and the two lines only differ in the transgene copy number. Furthermore, the corresponding genomic sequence on the other copy of Chr. 4 is WT. Rather, the spectrum of abnormalities in line-H transgenic mice is consistent with disruption of signaling by select BMPs during embryonic development or early growth. BMP signaling plays a key role in a wide range of physiological processes involved in both the development and homeostatic maintenance of various organs [28,38-40]. ERFE was also identified as a vascular morphogen in Xenopus embryos where it acts by antagonizing BMP4 [35]. Our observations raise the possibility that some of the nonhematologic complications experienced by patients with ineffective erythropoiesis [14-16] could either be caused or exacerbated by disrupted BMP signaling.

Specifically, deletion of *Bmp7* in mice leads to impaired embryonic kidney development [41,42]. Eye development is also regulated, in part, by BMP signaling [38,41] and disruption of BMP signaling by conditional deletion of BMP receptors in the eye during embryonic development leads to anophthalmia [43]. BMP4 is required for normal

vestibular function and BMP4$^{+/-}$ mice demonstrate circling behavior [40], similar to line-H transgenic mice in the present study. While mouse ERFE is reported to not inhibit BMP4 [35], ERFE may interact with and inhibit BMP4 heterodimers formed with other BMPs, e.g. BMP7 [44]. Adipogenesis is regulated by nuanced interplay between BMP signaling and antagonism [45,46]. A preferential effect of ERFE on visceral fat compared with subcutaneous fat, as the present study suggests, may be due to differences in the expression of, or receptivity to, specific BMPs by adipocytes or adipose progenitor cells in these compartments [47 48]. ERFE is reported to alter BMP2 signaling in a "depot-specific" manner *in vitro*, altering BMP signaling to a greater degree in adipocytes derived from some adipose compartments compared with others [49]. Reduced adiposity in response to *Erfe* overexpression is consistent with previous findings of increased adipose deposit size in *Erfe*-deficient mice [50].

Altered postnatal survival and decreased body weights were more prominent in male line-H *Erfe*-overexpressing mice compared with females, despite similar circulating ERFE levels between sexes. This difference in phenotype severity based on sex may be attributable to differences in basal, tissue-specific expression of BMPs between sexes, with female mice expressing greater levels of BMPs, driven by estrogen signaling [51,52], possibly compensating for BMP inhibition by ERFE.

A well-documented complication of β-thalassemia is a loss of bone mineral density associated with marrow expansion driven by chronic erythropoietic stimulation [53]. We observed no clear difference in steady-state bone histomorphometry between line-H *Erfe*-overexpressing mice and WT controls. The lack of effect of ERFE on bone development and mineralization was unexpected given the substantial effects, including spontaneous fractures, observed in bones of mice overexpressing other BMP antagonists [54,55]. However, in these studies BMP antagonists were overexpressed selectively in cells of the osteoblast lineage and likely exhibited autocrine inhibition of BMP signaling in osteoblasts, unlike in the present study where endocrine or paracrine BMP inhibition by ERFE predominated.

Kidney dysfunction in the context of β-thalassemia is incompletely understood but thought to result from a combination of iron-mediated damage, chronic anemia with renal hypoxia, and treatment with iron chelators that may damage the kidney [56]. Signaling by BMP7 is thought to protect against renal fibrosis [57] and increased expression of BMP antagonists may predispose the kidney to tubular injury [58], exacerbating damage from excess iron or chelation therapy. Reducing the amount or activity of ERFE in patients with β-thalassemia may represent a potential therapeutic option for preventing kidney damage. It remains to be determined which aspects of the phenotype observed in mice with high circulating ERFE levels in this study are the result of altered BMP signaling in utero versus during postnatal life. Relative to human β-thalassemia, transgenic mice in this study may be more susceptible to abnormal organ development because of differences in the timing of increased *Erfe* expression during embryonic and postnatal development. In humans with β-thalassemia, anemia and ineffective erythropoiesis does not develop until after birth [59] because of the protective effect of fetal hemoglobin, whereas transgene expression in our mouse model begins during embryonic development [21]. Therefore, increased *Erfe* expression, resulting from anemia in patients with β-thalassemia, is not expected until the postnatal period, diminishing the potential effects on organ development. However, elevated ERFE levels in utero would be expected in patients with fetal anemias such as α-thalassemia, pyruvate kinase deficiency, congenital dyserythropoietic anemia and other congenital anemias with ineffective erythropoiesis [59]. In particular, elevated ERFE could contribute to developmental abnormalities seen in patients with severe α-globin deficiency [60].

In conclusion, our mouse models demonstrate that chronically increased blood ERFE levels contribute to iron loading and, at high levels, alter the development or homeostasis of multiple organ systems. ERFE may be a suitable therapeutic target in anemias from ineffective erythropoiesis to reduce iron loading and possible organ dysfunction from ERFE-mediated inhibition of BMP signaling.

Acknowledgments

Support for this work was provided by NIH R01DK126680 (TG) and Cooley's Anemia Foundation (RC). The authors thank the UCLA Translational Pathology Core Laboratory for histology processing, the UCLA

Technology Center for Genomics & Bioinformatics (TCGB) for performing genomic sequencing, and the UCLA Behavioral Testing Core for performing mouse behavioral analysis.

Author Contributions

RC designed and performed experiments, analyzed data, and wrote the manuscript. GJ performed experiments and assisted with data interpretation. RCP performed bone analyses and assisted with their interpretation. EN and TG conceived the project, designed experiments, analyzed data, and wrote the manuscript.

Declaration of Interests

TG and EN are scientific co-founders of Intrinsic LifeSciences and Silarus Pharma. TG is a consultant for ADARx, Akebia, Pharmacosmos, Ionis, Gossamer Bio, Global Blood Therapeutics, American Regent, Disc Medicine, and Rockwell Scientific. EN is a consultant for Protagonist, Ionis and Disc Medicine. TG and EN are inventors on patents related to erythroferrone. RC, RCP and GJ declare no conflicts.

References

1. Nemeth E, Tuttle MS, Powelson J, et al. Hepcidin regulates cellular iron efflux by binding to ferroportin and inducing its internalization. *Science*. 2004;306(5704):2090-2093.

2. Liu Q, Davidoff O, Niss K, Haase VH. Hypoxia-inducible factor regulates hepcidin via erythropoietin-induced erythropoiesis. *J Clin Invest*. 2012;122(12):4635-4644.

3. Jones E, Pasricha SR, Allen A, et al. Hepcidin is suppressed by erythropoiesis in hemoglobin E beta-thalassemia and beta-thalassemia trait. *Blood*. 2015;125(5):873-880.

4. Kearney SL, Nemeth E, Neufeld EJ, et al. Urinary hepcidin in congenital chronic anemias. *Pediatr Blood Cancer*. 2007;48(1):57-63.

5. Pak M, Lopez MA, Gabayan V, Ganz T, Rivera S. Suppression of hepcidin during anemia requires erythropoietic activity. *Blood*. 2006;108(12):3730-3735.

6. Kautz L, Jung G, Valore EV, Rivella S, Nemeth E, Ganz T. Identification of erythroferrone as an erythroid regulator of iron metabolism. *Nat Genet*. 2014;46(7):678-684.

7. Arezes J, Foy N, McHugh K, et al. Erythroferrone inhibits the induction of hepcidin by BMP6. *Blood*. 2018;132(14):1473-1477.

8. Wang CY, Xu Y, Traeger L, et al. Erythroferrone lowers hepcidin by sequestering BMP2/6 heterodimer from binding to the BMP type I receptor ALK3. *Blood*. 2020;135(6):453-456.

9. Koch PS, Olsavszky V, Ulbrich F, et al. Angiocrine Bmp2 signaling in murine liver controls normal iron homeostasis. *Blood*. 2017;129(4):415-419.

10. Canali S, Zumbrennen-Bullough KB, Core AB, et al. Endothelial cells produce bone morphogenetic protein 6 required for iron homeostasis in mice. *Blood*. 2017;129(4):405-414.

11. Arezes J, Foy N, McHugh K, et al. Antibodies against the erythroferrone N-terminal domain prevent hepcidin suppression and ameliorate murine thalassemia. *Blood*. 2020;135(8):547-557.

12. Ganz T, Jung G, Naeim A, et al. Immunoassay for human serum erythroferrone. *Blood*. 2017;130(10):1243-1246.

13. Papakonstantinou O, Alexopoulou E, Economopoulos N, et al. Assessment of iron distribution between liver, spleen, pancreas, bone marrow, and myocardium by means of R2 relaxometry with MRI in patients with beta-thalassemia major. *J Magn Reson Imaging*. 2009;29(4):853-859.

14. Musallam KM, Taher AT. Mechanisms of renal disease in beta-thalassemia. *J Am Soc Nephrol*. 2012;23(8):1299-1302.

15. Rodda CP, Reid ED, Johnson S, Doery J, Matthews R, Bowden DK. Short stature in homozygous beta-thalassaemia is due to disproportionate truncal shortening. *Clin Endocrinol (Oxf)*. 1995;42(6):587-592.

16. Karimi M, Ghiam AF, Hashemi A, Alinejad S, Soweid M, Kashef S. Bone mineral density in beta-thalassemia major and intermedia. *Indian Pediatr*. 2007;44(1):29-32.

17. Kautz L, Jung G, Nemeth E, Ganz T. Erythroferrone contributes to recovery from anemia of inflammation. *Blood*. 2014;124(16):2569-2574.

18. Kautz L, Jung G, Du X, et al. Erythroferrone contributes to hepcidin suppression and iron overload in a mouse model of beta-thalassemia. *Blood*. 2015;126(17):2031-2037.

19. Coffey R, Sardo U, Kautz L, Gabayan V, Nemeth E, Ganz T. Erythroferrone is not required for the glucoregulatory and hematologic effects of chronic erythropoietin treatment in mice. *Physiol Rep*. 2018;6(19):e13890.

20. Suresh S, Rajvanshi PK, Noguchi CT. The Many Facets of Erythropoietin Physiologic and Metabolic Response. *Front Physiol*. 2019;10:1534.

21. Peterson KR, Fedosyuk H, Zelenchuk L, et al. Transgenic Cre expression mice for generation of erythroid-specific gene alterations. *Genesis*. 2004;39(1):1-9.

22. Dempster DW, Compston JE, Drezner MK, et al. Standardized nomenclature, symbols, and units for bone histomorphometry: a 2012 update of the report of the ASBMR Histomorphometry Nomenclature Committee. *J Bone Miner Res*. 2013;28(1):2-17.

23. Courselaud B, Troadec MB, Fruchon S, et al. Strain and gender modulate hepatic hepcidin 1 and 2 mRNA expression in mice. *Blood Cells Mol Dis*. 2004;32(2):283-289.

24. Ramos E, Kautz L, Rodriguez R, et al. Evidence for distinct pathways of hepcidin regulation by acute and chronic iron loading in mice. *Hepatology*. 2011;53(4):1333-1341.

25. Corradini E, Meynard D, Wu Q, et al. Serum and liver iron differently regulate the bone morphogenetic protein 6 (BMP6)-SMAD signaling pathway in mice. *Hepatology*. 2011;54(1):273-284.

26. Mishina Y, Starbuck MW, Gentile MA, et al. Bone morphogenetic protein type IA receptor signaling regulates postnatal osteoblast function and bone remodeling. *J Biol Chem*. 2004;279(26):27560-27566.

27. Tsuji K, Bandyopadhyay A, Harfe BD, et al. BMP2 activity, although dispensable for bone formation, is required for the initiation of fracture healing. *Nat Genet*. 2006;38(12):1424-1429.

28. Bandyopadhyay A, Tsuji K, Cox K, Harfe BD, Rosen V, Tabin CJ. Genetic analysis of the roles of BMP2, BMP4, and BMP7 in limb patterning and skeletogenesis. *PLoS Genet*. 2006;2(12):e216.

29. Gardenghi S, Marongiu MF, Ramos P, et al. Ineffective erythropoiesis in beta-thalassemia is characterized by increased iron absorption mediated by down-regulation of hepcidin and up-regulation of ferroportin. *Blood*. 2007;109(11):5027-5035.

30. McCranor BJ, Langdon JM, Prince OD, et al. Investigation of the role of interleukin-6 and hepcidin antimicrobial peptide in the development of anemia with age. *Haematologica*. 2013;98(10):1633-1640.

31. Hanudel MR, Rappaport M, Gabayan V, et al. Increased serum hepcidin contributes to the anemia of chronic kidney disease in a murine model. *Haematologica*. 2017;102(3):e85-e88.

32. Gardenghi S, Ramos P, Marongiu MF, et al. Hepcidin as a therapeutic tool to limit iron overload and improve anemia in beta-thalassemic mice. *J Clin Invest*. 2010;120(12):4466-4477.

33. Casu C, Oikonomidou PR, Chen H, et al. Minihepcidin peptides as disease modifiers in mice affected by beta-thalassemia and polycythemia vera. *Blood*. 2016;128(2):265-276.

34. Andolfo I, Rosato BE, Marra R, et al. The BMP-SMAD pathway mediates the impaired hepatic iron metabolism associated with the ERFE-A260S variant. *Am J Hematol*. 2019;94(11):1227-1235.

35. Melchert J, Henningfeld KA, Richts S, Lingner T, Jonigk D, Pieler T. The secreted BMP antagonist ERFE is required for the development of a functional circulatory system in Xenopus. *Dev Biol*. 2020;459(2):138-148.

36. Korchynskyi O, ten Dijke P. Identification and functional characterization of distinct critically important bone morphogenetic protein-specific response elements in the Id1 promoter. *J Biol Chem*. 2002;277(7):4883-4891.

37. Mleczko-Sanecka K, Casanovas G, Ragab A, et al. SMAD7 controls iron metabolism as a potent inhibitor of hepcidin expression. *Blood*. 2010;115(13):2657-2665.

38. Dudley AT, Lyons KM, Robertson EJ. A requirement for bone morphogenetic protein-7 during development of the mammalian kidney and eye. *Genes Dev*. 1995;9(22):2795-2807.

39. Yoon BS, Ovchinnikov DA, Yoshii I, Mishina Y, Behringer RR, Lyons KM. Bmpr1a and Bmpr1b have overlapping functions and are essential for chondrogenesis in vivo. *Proc Natl Acad Sci U S A*. 2005;102(14):5062-5067.

40. Blauwkamp MN, Beyer LA, Kabara L, et al. The role of bone morphogenetic protein 4 in inner ear development and function. *Hear Res*. 2007;225(1-2):71-79.

41. Karsenty G, Luo G, Hofmann C, Bradley A. BMP 7 is required for nephrogenesis, eye development, and skeletal patterning. *Ann N Y Acad Sci*. 1996;785:98-107.

42. Luo G, Hofmann C, Bronckers AL, Sohocki M, Bradley A, Karsenty G. BMP-7 is an inducer of nephrogenesis, and is also required for eye development and skeletal patterning. *Genes Dev*. 1995;9(22):2808-2820.

43. Murali D, Yoshikawa S, Corrigan RR, et al. Distinct developmental programs require different levels of Bmp signaling during mouse retinal development. *Development*. 2005;132(5):913-923.

44. Kim HS, Neugebauer J, McKnite A, Tilak A, Christian JL. BMP7 functions predominantly as a heterodimer with BMP2 or BMP4 during mammalian embryogenesis. *Elife*. 2019;8.

45. Blazquez-Medela AM, Jumabay M, Rajbhandari P, et al. Noggin depletion in adipocytes promotes obesity in mice. *Mol Metab*. 2019;25:50-63.

46. Gustafson B, Hammarstedt A, Hedjazifar S, et al. BMP4 and BMP Antagonists Regulate Human White and Beige Adipogenesis. *Diabetes*. 2015;64(5):1670-1681.

47. Guiu-Jurado E, Unthan M, Bohler N, et al. Bone morphogenetic protein 2 (BMP2) may contribute to partition of energy storage into visceral and subcutaneous fat depots. *Obesity (Silver Spring)*. 2016;24(10):2092-2100.

48. Macotela Y, Emanuelli B, Mori MA, et al. Intrinsic differences in adipocyte precursor cells from different white fat depots. *Diabetes*. 2012;61(7):1691-1699.

49. Denton NF, Eghleilib M, Al-Sharifi S, et al. Bone morphogenetic protein 2 is a depot-specific regulator of human adipogenesis. *Int J Obes (Lond)*. 2019;43(12):2458-2468.

50. Little HC, Rodriguez S, Lei X, et al. Myonectin deletion promotes adipose fat storage and reduces liver steatosis. *FASEB J*. 2019;33(7):8666-8687.

51. Ong DB, Colley SM, Norman MR, Kitazawa S, Tobias JH. Transcriptional regulation of a BMP-6 promoter by estrogen receptor alpha. *J Bone Miner Res*. 2004;19(3):447-454.

52. Zhou S, Turgeman G, Harris SE, et al. Estrogens activate bone morphogenetic protein-2 gene transcription in mouse mesenchymal stem cells. *Mol Endocrinol*. 2003;17(1):56-66.

53. Tyler PA, Madani G, Chaudhuri R, Wilson LF, Dick EA. The radiological appearances of thalassaemia. *Clin Radiol*. 2006;61(1):40-52.

54. Devlin RD, Du Z, Pereira RC, et al. Skeletal Overexpression of Noggin Results in Osteopenia and Reduced Bone Formation. *Endocrinology*. 2003;144(5):1972-1978.

55. Gazzerro E, Pereira RC, Jorgetti V, Olson S, Economides AN, Canalis E. Skeletal overexpression of gremlin impairs bone formation and causes osteopenia. *Endocrinology*. 2005;146(2):655-665.

56. Demosthenous C, Vlachaki E, Apostolou C, et al. Beta-thalassemia: renal complications and mechanisms: a narrative review. *Hematology*. 2019;24(1):426-438.

57. Zeisberg M, Bottiglio C, Kumar N, et al. Bone morphogenic protein-7 inhibits progression of chronic renal fibrosis associated with two genetic mouse models. *Am J Physiol Renal Physiol*. 2003;285(6):F1060-1067.

58. Yanagita M, Okuda T, Endo S, et al. Uterine sensitization-associated gene-1 (USAG-1), a novel BMP antagonist expressed in the kidney, accelerates tubular injury. *J Clin Invest*. 2006;116(1):70-79.

59. Blobel GA, Bodine D, Brand M, et al. An international effort to cure a global health problem: A report on the 19th Hemoglobin Switching Conference. *Exp Hematol*. 2015;43(10):821-837.

60. Songdej D, Babbs C, Higgs DR, Consortium BI. An international registry of survivors with Hb Bart's hydrops fetalis syndrome. *Blood*. 2017;129(10):1251-1259.